Journal of Astronomical Instrumentation, Vol. 7, No. 4 (2018) 1840003 (14 pages)
© The Author(s)
DOI: 10.1142/S2251171718400032

J. Astron. Instrum. 2018.07. Downloaded from www.worldscientific.com
by GERMAN AEROSPACE CENTER (DLR) on 01/09/19. Re-use and distribution is strictly not permitted, except for Open Access articles.

FIFI-LS: The Field-Imaging Far-Infrared Line Spectrometer on SOFIA

Christian Fischer[1,12], Simon Beckmann[1], Aaron Bryant[2], Sebastian Colditz[1], Fabio Fumi[2], Norbert Geis[3], Mourad Hamidouche[4], Thomas Henning[5], Rainer Hönle[2], Christof Iserlohe[1], Randolf Klein[6], Alfred Krabbe[1,2], Leslie Looney[7], Albrecht Poglitsch[3], Walfried Raab[8], Felix Rebell[2], Dirk Rosenthal[9], Maureen Savage[10,6], Mario Schweitzer[11], Christopher Trinh[6] and William Vacca[6]

[1]Deutsches SOFIA Institut
University of Stuttgart, 70569 Stuttgart, Germany

[2]Institute of Space Systems
University of Stuttgart, 70569 Stuttgart, Germany

[3]Max Planck Institute for Extraterrestrial Physics
85748 Garching, Germany

[4]Remote Sensing Technology Institute
DLR (German Aerospace Center)
82234 Wessling, Germany

[5]Max Planck Institute for Astronomy
69117 Heidelberg, Germany

[6]SOFIA-USRA, NASA Ames Research Center
Moffett Field, CA, 94035, USA

[7]Department of Astronomy, University of Illinois
Urbana, IL, 61801, USA

[8]ESTEC, European Space Agency, 69117, Nordwijk
2201 AZ, The Netherlands

[9]OSRAM GmbH, Industriestraße 20B
85072 Eichstätt, Germany

[10]UC Observatories, 1156 High Street
Santa Cruz, CA, 95064, USA

[11]OHB System AG, 82234 Wessling, Germany
[12]fischer@dsi.uni-stuttgart.de

Received April 14, 2018; Accepted June 18, 2018; Published July 20, 2018

We describe the design of the Field-Imaging Far-Infrared Line Spectrometer (FIFI-LS), operated as a Facility-Class instrument on the Stratospheric Observatory for Infrared Astronomy (SOFIA). FIFI-LS is an imaging spectrometer for medium resolution spectroscopy. Since being commissioned in 2014, it has performed over 50 SOFIA commissioning and science flights. After operating as a principal investigator instrument in 2014 and early 2015, it was accepted as a Facility Science Instrument in 2015. In addition to the description of the design, we report on the in-flight performance and the concept of operation. We also provide an overview of the science opportunities with FIFI-LS and describe how FIFI-LS observations complement and complete observations with the PACS instrument on the Herschel observatory.

Keywords: Integral field spectroscopy, spectrometer, far-Infrared, FIFI-LS, SOFIA.

[12]Corresponding author.
This is an Open Access article published by World Scientific Publishing Company. It is distributed under the terms of the Creative Commons Attribution 4.0 (CC-BY) License. Further distribution of this work is permitted, provided the original work is properly cited.

J. Astron. Instrum. 2018.07. Downloaded from www.worldscientific.com
by GERMAN AEROSPACE CENTER (DLR) on 01/09/19. Re-use and distribution is strictly not permitted, except for Open Access articles.

1. Introduction

The Field-Imaging Far-Infrared Line Spectrometer (FIFI-LS) is a far-infrared integral field spectrograph designed for observations on the Stratospheric Observatory for Infrared Astronomy (SOFIA; Erickson & Davidson, 1993). The first observations with FIFI-LS on SOFIA were obtained in March 2014 and to date the instrument has been operated on more than 50 SOFIA science and commissioning flights. The FIFI-LS instrument features two parallel spectral channels with wavelength ranges of 51–125 μm ("blue channel") and 115–203 μm ("red channel"), respectively, that can be operated simultaneously. Each channel has a field of view (FOV) consisting of 5 by 5 spatial pixels with a plate scale of 6 arc sec/pixel in the blue channel and 12 arc sec/pixel in the red channel. The spectral resolution of the instrument is in the range of $R \approx 500$ to ~ 2000 with an instantaneous coverage between 800 km/s and 3000 km/s.The combination of wavelength range and coverage, spectral resolution and imaging capabilities implies that FIFI-LS is particularly useful for investigations of the interstellar medium in our own and other galaxies.

Development of FIFI-LS began in 1997 at the Max Planck Institute for Extraterrestrial Physics (MPE) in Garching, Germany. It was originally designed to be a Principal Investigator (PI)-instrument. In 2010, the development was terminated at MPE due to a shift in scientific objectives. However, reviews by both NASA and DLR emphasized the scientific potential of FIFI-LS and in 2012 the instrument was transferred to the Institute of Space Systems (IRS) in Stuttgart to finish the development and characterization. The instrument was then commissioned aboard SOFIA in the spring of 2014 and was accepted by the SOFIA program as a Facility Science Instrument (FSI) in 2015.

FIFI-LS has a design and capabilities similar to those of the PACS instrument (Poglitsch *et al.*, 2010) onboard the *Herschel* satellite. FIFI-LS complements and builds on PACS observations while also enabling new science investigations with additional wavelength coverage and with the superior mapping capabilities of SOFIA.

In Fig. 1, a line flux map for the [OI] line at 145.5 μm in NGC2024 is shown together with the corresponding continuum flux map as an example for data obtained with FIFI-LS.

2. Science Opportunities

FIFI-LS on SOFIA plays a major role in investigations of star formation (primarily massive) and the interstellar medium in both our own galaxy and external galaxies. With its sensitivity, the latter topic is a prime capability of FIFI-LS on SOFIA. The spatial resolution of FIFI-LS is a huge improvement over available data from ISO (Kessler *et al.*, 1996) and allows to spatially resolve extragalactic sources, such as M82, better. The key features that FIFI-LS observes are the bright far-Infrared fine structure lines, e.g. [OI] 63 μm and 146 μm, [OIII] 52 μm and 88 μm, [NII] 122 μm, [NIII] 57 μm, [CII] 158 μm, and molecular lines like CO lines between $J = 13$–12 and $J = 38$–37. An overview of lines observed with FIFI-LS to date is given in Table 1.

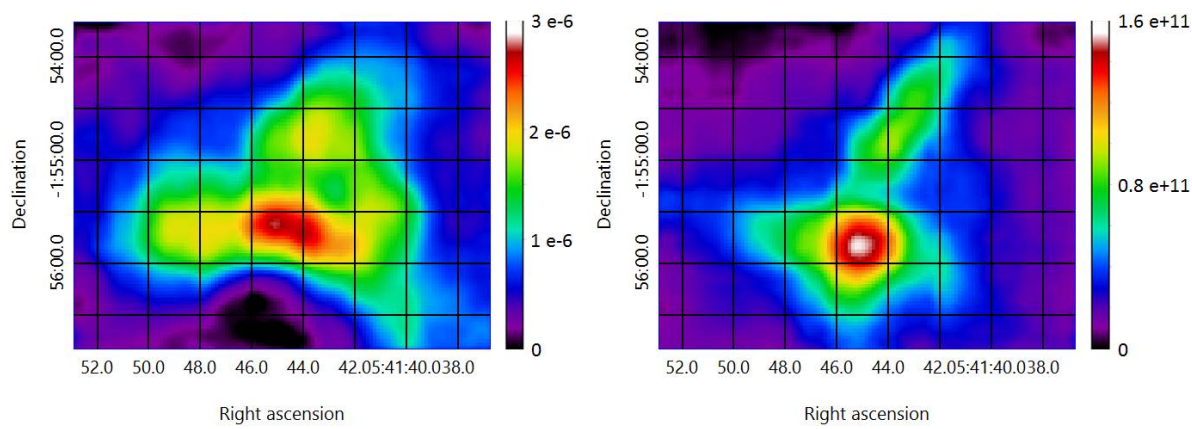

Fig. 1. [OI] at 145.525 μm in NGC 2024 as an example for FIFI-LS/SOFIA data. Left: Integrated line flux obtained with a Gaussian fit in W m^{-2} Sr^{-1}. Right: Continuum flux obtained with a first-order polynomial fit in Jy Sr^{-1}.

J. Astron. Instrum. 2018.07. Downloaded from www.worldscientific.com
by GERMAN AEROSPACE CENTER (DLR) on 01/09/19. Re-use and distribution is strictly not permitted, except for Open Access articles.

Table 1. Spectral lines already observed with FIFI-LS.

Line	λ [μm]	Line	λ [μm]	Line	λ [μm]	Line	λ [μm]
[OIII]	51.8	CH_4	80.1	CO	104.4	CO	162.8
OH	55.9	CO	84.4	CO	118.6	OH	163.3
[NIII]	57.3	OH	84.5	[NII]	122	HCN	169.4
[OI]	63.2	CO_2 (ice)	86	CO	124.2	CO	174
C_2H_2	68.6	CO	87.2	CO	130.4	CO	186
CO	69.1	CH_4	87.3	[OI]	145.5	CO	200.3
C_2H_2	69.7	[OIII]	88.4	CO_2 (ice)	146		
CO	70.9	OH	96.3	CO	153.3		
CO	77.1	CO	96.8	[CII]	157.7		

2.1. *Typical use cases*

One typical application of FIFI-LS is obtaining maps of [CII] emission in nearby galaxies. Large maps of [CII] emission in nearby galaxies like M51 and NGC6946 have been obtained in 10–15 h of observing time. An area of 60 arc min^2 can be integrated to reach a noise level of 10^{-17} W/m^2 per spatial pixel ("spaxel", 12×12 arc sec^2) in about 15 h of wall clock time. For smaller sources that fit into 1×1 arc min^2 FOV of the red channel, deep integrations are easily possible. [CII] has been detected in sources with red shifts of up to 0.04 in wall clock times below two hours.

The oxygen lines [OI] at 63 μm and 146 μm are also frequently observed simultaneously with FIFI-LS as they play a major role in the analysis of photo-dissociation regions (PDRs). The line flux ratio provides constraints on the density and the UV flux in the region. In addition, FIFI-LS observations of the relatively weak [OI] line at 146 μm (typically a few times weaker than the [OI] 63 μm line) are essential as a diagnostic of the conditions within the PDR since the often used line at 63 μm can be optically thick for many sources. When mapping extended sources with multiple FOVs in the blue channel (30×30 arc sec^2), the red channel gets four times the integration time due to the overlap created by its larger size (1×1 arc min^2). This helps to detect the fainter line in the red channel. So mapping both [OI] lines simultaneously with FIFI-LS is frequently carried out.

The line pair of [OIII] at 52 μm and 88 μm is very valuable for the analysis of HII regions since the ratio probes the electron density in the region. With the addition of the also available [NIII] line at 57 μm, it is also possible to probe the metallicity (Nagao *et al.*, 2011). FIFI-LS observations of the [OIII] line at 52 μm and the [NIII] line at 57 μm are frequently obtained to fully utilize existing data sets of other spectral lines obtained with PACS at similar spatial resolution.

Using the quickly movable SOFIA telescope, large maps of bright galactic regions can be obtained very efficiently. With the FIFI-LS "bright object mode", a 32.5 arc min^2 map of the Orion BN/KL region in the [CII] 158 μm and [OI] 63 μm lines was completed in 76 min. In the region around the Circumnuclear Ring (CNR) at the galactic center (Iserlohe *et al.*, 2018), a deep map of about 136 arc min^2 was executed in a total time of about 5 hours.

Another unique capability of FIFI-LS is the efficient mapping of high J CO lines. Such maps have been successfully produced for the BN/KL (Looney *et al.*, 2018) as well as the CNR regions. The sensitivity of FIFI-LS enables the study of fainter sources like protostars as well.

3. Instrument Description

3.1. *Imaging spectroscopy*

FIFI-LS is an imaging spectrometer. As such, it allows the observation of spectra at every spatial pixel in a two-dimensional (2D) FOV in a single observation. Therefore, imaging spectroscopy is often referred to as 3D spectroscopy. An overview of how imaging spectroscopy is carried out with FIFI-LS is given in Fig. 2. After the light from the telescope is separated into the red and blue channels by a dichroic, the 5×5 spaxels are rearranged into a pseudo slit of 25 spaxels, with four gaps, that later help to separate the spaxels on the detector. The light is then dispersed on the two gratings and projected onto the 25×16 pixel detectors.

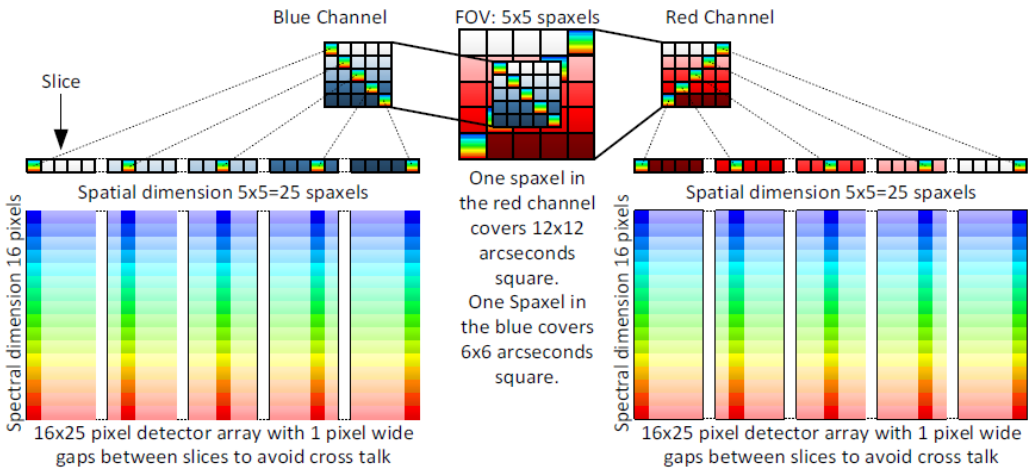

Fig. 2. Schematic of the FIFI-LS concept for imaging spectroscopy. The blue and red channel observations overlap on the sky, split internally by the entrance optics. The FOV of 5 × 5 spaxels in each channel is rearranged into a pseudo slit of 25 spaxels (and 4 gap-spaxels). This slit is dispersed with the gratings onto the 25 by 16 pixel detectors. One of the 5 spaxels in each slice is highlighted to show how the light is distributed on the detector.

3.2. *Instrument design*

A picture of the instrument installed on the SOFIA telescope, as well as a drawing of the cryostat installed at the telescope flange, are provided in Fig. 3. The cryostat (gray) sits on top of a cradle (also gray). A pressure coupler (orange) operates as a pressure barrier for the aircraft cabin, since stratospheric pressure prevails inside the telescope tub during flight.

The instrument operates at four temperature levels. The bore sight box, which houses the warm dichroic is at room temperature and stratospheric pressure. Inside the vacuum vessel there are three temperature levels: "nitrogen" (red), "helium" (blue) and "superfluid helium" (magenta), realized with three cryogen tanks. For each tank there is a neck assembly with redundant vent paths to ensure safe venting of the boiled-off cryogens during normal operation, as well as in case of a loss-of-vacuum event in the cryostat.

A schematic overview of the complete optical path of FIFI-LS is presented in Fig. 4. A detailed overview over the optical design of the instrument is available in Looney *et al.* (2000) and Raab *et al.* (2003). The light coming from the telescope through the Nasmyth tube is reflected into the FIFI-LS cryostat at the "Warm Dichroic". Currently, a fully reflective mirror is installed at that location. The

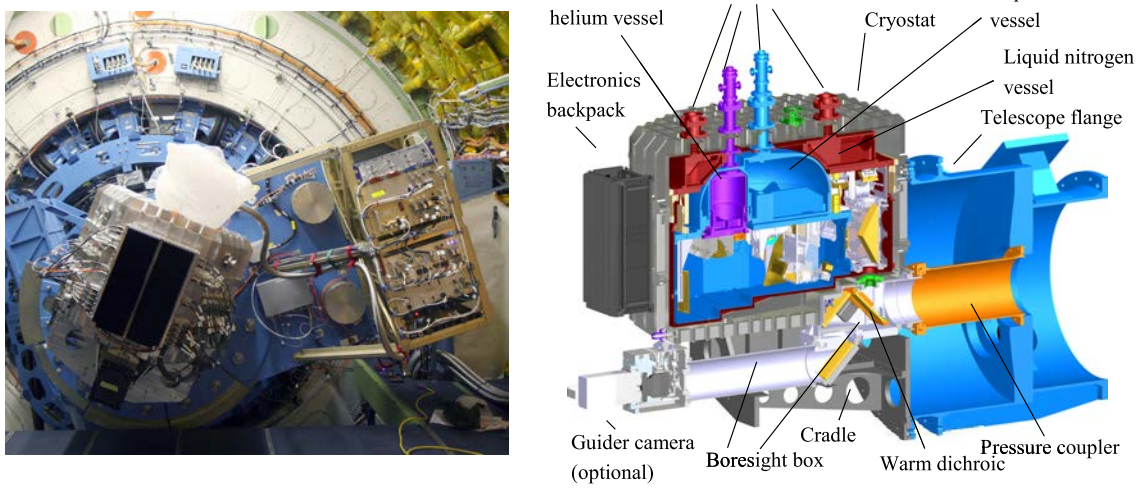

Fig. 3. Left: FIFI-LS and its counter weight rack (CWR) installed at the SOFIA telescope. The telescope is at the lower end of its 20–60° elevation range. Right: A drawing of FIFI-LS with some main components labeled.

J. Astron. Instrum. 2018.07. Downloaded from www.worldscientific.com
by GERMAN AEROSPACE CENTER (DLR) on 01/09/19. Re-use and distribution is strictly not permitted, except for Open Access articles.

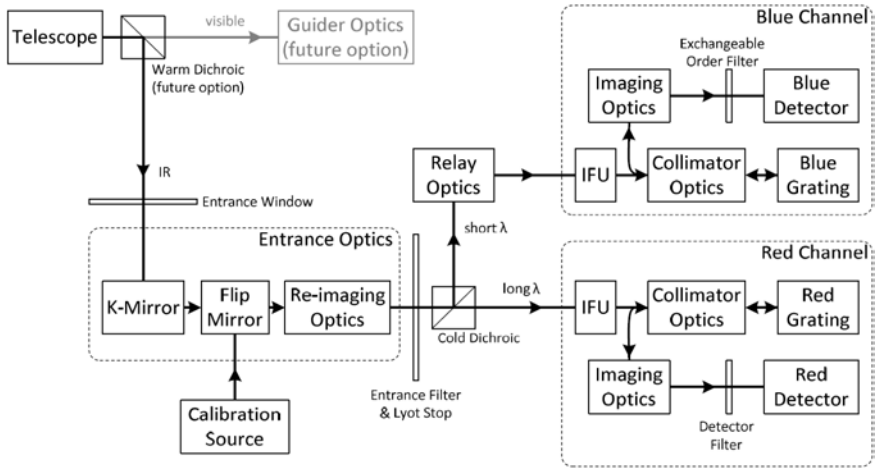

Fig. 4. Schematic of the FIFI-LS optical path from the telescope to the detectors of both channels.

optional instrument guider optics plus guiding camera originally planned for that location have not been implemented since the guiding provided by the telescope has proven sufficient for maintaining the FIFI-LS image quality close to the diffraction limit. The fully reflective mirror rests on a stage that permits rotation in two axes. Since the mirror is located close to a focus in the optical path, it is used for pupil alignment of the instrument. Pupil alignment was performed on the SOFIA facilities Telescope Assembly Alignment Simulator (Thompson, 2011). The incoming light is then transmitted through the entrance window that forms the pressure boundary of the cryostat. The entrance optics are located on the nitrogen plate. A K-mirror is used to rotate the quadratic footprint on the sky to optimize the coverage for sources as well as to keep the field orientation fixed on the detectors throughout long integrations while the sky rotates relative to the telescope. More details can be found in Colditz *et al.* (2014). A flip mirror is used to switch the optical path between the sky and a calibration source. The calibration source itself is thermally connected to the helium optical bench, but located outside of the helium shield. It contains an electrically heated radiator, an integrating sphere and a chopper to generate signal levels comparable to that from the sky (Schweitzer *et al.*, 2008; Rebell, 2018). It is used to generate spectral and spatial flat fields. The LN_2 plate also houses several motors for the diffraction grating coarse drives and the dichroic filter changer on the LHe plate. Transfer of the motion through the helium shield is effected via magnetic coupling.

The light enters the helium cooled optical plate through the Lyot stop and the entrance filter assembly. The filter has a short wavelength cut off at $\sim 40\,\mu$m. On the LHe plate the light is first split up into the blue and red channels by the cold dichroic. This is a mesh dichroic that transmits the longer wavelength for the red channel and reflects the light for the blue channel. Since the transition between transmission and reflection is not a perfect step function at a single wavelength but extends over several microns, two interchangeable dichroics are available to maintain full wavelength coverage in both channels. The dichroics also provide some flexibility in the channel in which a specific wavelength is to be observed. For example, the CO line at $\sim 119\,\mu$m can be observed in either the blue or the red channel.

The integral field units (IFU) rearrange the 5×5 spaxel FOV into the 25 spaxel pseudo slit (see Sec. 3.1) that is projected onto the diffraction gratings *via* the collimator optics. The instantaneous wavelength range covered by the detector is set by rotating the gratings with a multi-stage drive in a nested control loop. More details on the grating systems can be found in Rebell *et al.* (2014) and Rebell (2018). The beam passes through the collimator optics for the second time on its way to the detectors. In the blue channel, observations are performed in both first and second order and an interchangeable filter is located in that channel on the LHe plate before the light enters the detector assembly. The motor running that filter changer is the only motor operating on the LHe plate. In operation, the plate typically reaches a temperature of about 6° K.

J. Astron. Instrum. 2018.07. Downloaded from www.worldscientific.com by GERMAN AEROSPACE CENTER (DLR) on 01/09/19. Re-use and distribution is strictly not permitted, except for Open Access articles.

J. Astron. Instrum. 2018.07. Downloaded from www.worldscientific.com
by GERMAN AEROSPACE CENTER (DLR) on 01/09/19. Re-use and distribution is strictly not permitted, except for Open Access articles.

The detector assembly is cooled by helium pumped down to about 20 m bar to operate at a temperature of about 1.8°K. FIFI-LS uses gallium-doped germanium pixels in both channels. The spectral sensitivity of gallium-doped germanium pixels is high between $\sim 40\,\mu$m and $\sim 120\,\mu$m, ideal for the blue channel. For the spectral range of the red channel the detector elements are compressed in their mounting structures in order to shift the area of good spectral sensitivity into the wavelength range of $\sim 120\,\mu$m to $\sim 210\,\mu$m (Rosenthal *et al.*, 2000). The pixels in the blue channel have a size of 6×6 arc sec^2 on the sky and in the red channel the projected size is 12×12 arc sec^2; the plate scales were chosen to roughly match the diffraction-limited point spread functions at the mean wavelengths of the two channels. Having two detectors operating in parallel also enables FIFI-LS to map two lines simultaneously, which is a multiplex advantage on an airborne observatory operating a limited number of science hours per year.

3.3. *Electronics*

The arrangement of the electronics for FIFI-LS reflects the arrangement of the instrument at the telescope in the aircraft. An overview showing the signal connections between the locations is provided in Fig. 5.

Instrument operation is performed at the PI rack, which holds three computers and two terminals to allow two operators to control and monitor the instrument in parallel. The MASTER computer runs the main user interface for the instrument control. It controls the observation process based on scripted parameters, by distributing commands and data to the other machines in the system and monitoring their feedback. The MIDDLEMAN computer provides the interface to the SOFIA telescope, receiving the commands from MASTER and translating them into commands that are used to control the SOFIA telescope. It also monitors the telescope's status and relays any information important for an observation, e.g. telescope errors, to MASTER. The MAKER computer records the digitized observational data and forwards it via the on-board computer network to a storage disk, where it may be reduced, viewed and analyzed by the scientists on board the SOFIA and used to make real-time observation planning decisions.

The counter weight rack (CWR) is located at the telescope assembly close to the instrument flange (see Fig. 3). It contains electronics that must be close to the instrument to ensure good signal quality. The MOTHER computer controls the mechanisms in the cryostat and the detector readout timing by generating a set of high level clock

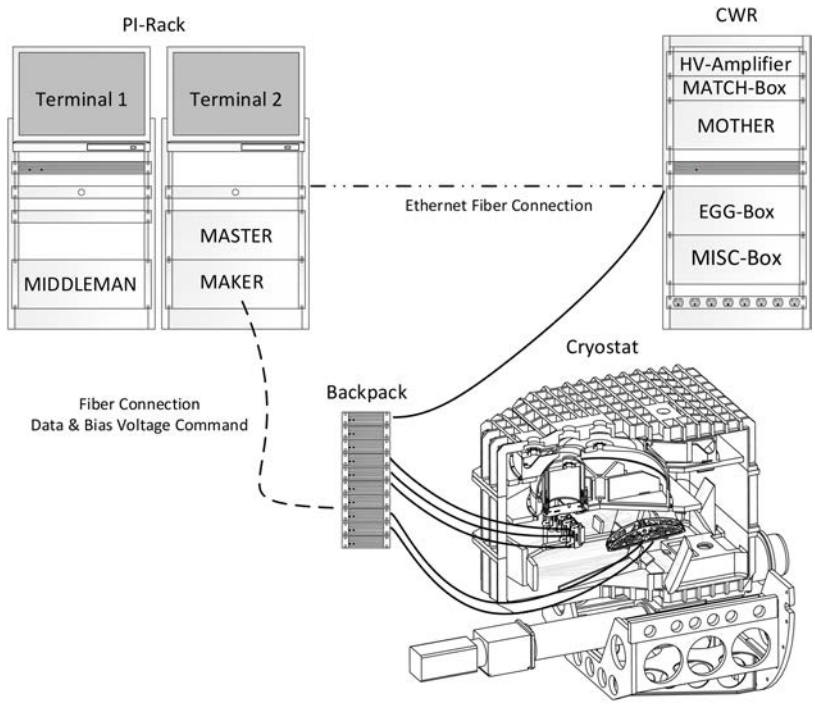

Fig. 5. Overview over the electronics layout of FIFI-LS.

J. Astron. Instrum. 2018.07. Downloaded from www.worldscientific.com
by GERMAN AEROSPACE CENTER (DLR) on 01/09/19. Re-use and distribution is strictly not permitted, except for Open Access articles.

signals. In the EGG-Box two PC104 Stacks ("red" and "blue" EMBRYO) control the coarse drives for the gratings and command the driving voltages (which are amplified by the HV-Amplifier) of the piezo stacks of the fine drive. The grating positions are controlled using digital PID feedback loops running on the EMBRYO machines to reduce oscillations of the gratings. The MISC-Box contains the low-level controllers for the mechanisms, excluding the grating drives. A temperature display for the different zones in the cryostat is available in the MATCH-Box. Electronics that need to be located very close to the cryostat in order to avoid noise on analogue data lines were built into the electronics BACKPACK. The BACKPACK is directly attached to the rear of the cryostat and is built symmetrically, having the same set of electronics boards for the blue and for the red channel. Tasks performed here include the digitization and relay of the detector and grating position readouts, and providing power and clock signals for the detectors, as well as bias voltages.

The cryostat contains the detector readout electronics, operating at $\sim$1.8°K. The cold readout electronics (CREs) were developed for the PACS instrument. The CREs amplify the voltage measurements and relay the amplified signal to a set of warm pre-amplifiers located on the inner wall of the cryostat shell. After amplification, the signals are relayed to the BACKPACK for digitization. The cryostat also contains the motors and actuators for the mechanisms, the respective end switches of these mechanisms, as well as the Inductosyn® rotary transducers used to measure the positions of the red and blue gratings.

3.4. *Software*

The instrument uses information stored in script files called "scan descriptions" to command the internal mechanisms and the telescope during an observation. Each scan description defines a short observation and contains information like the position of the observed target, the integration times for the detectors, the chopping frequency for the secondary mirror and the wavelengths to be observed. A set of multiple scan descriptions is necessary to define and execute a complete astronomical observation including nods. This sequence of scan descriptions is, in turn, stored in a schedule file, which is completed sequentially by the instrument software. More details on the generation of the scan descriptions can be found in Bryant *et al.* (2014).

Multiple processes then run the instrument, with "fifimain" being the major one. This process reads the current scan description according to the schedule file. The information is then evaluated and distributed to the other processes in the system using the inter-process communication protocol kosma_io, which is part of the KOSMA-control software package also used by the GREAT instrument (Guesten *et al.*, 2003). More details on the processes can be found in Klein *et al.* (2004). Communication with the telescope is maintained via the KOSMA_translator (Stutzki, 2004), which converts the telescope commands from the FIFI-LS instrument (conforming to the KOSMA-control software) into commands that may be executed by the telescope's Mission Controls and Communications System (MCCS).

The astronomical data are processed by a dedicated pipeline that reduces the data obtained during an entire observation, beginning with the time-resolved raw values, into a single cube (two spatial dimensions and one spectral dimension) comprising a map that can be used for astronomical analysis. The pipeline has been implemented in IDL in the observatory's "Redux" environment, which unifies the pipeline development efforts across SOFIA's suite of instruments as well as with the instrument team (Clarke *et al.*, 2015). The instrument records the cumulative signal detected every 1/250 s. The sequence of cumulative signal values as a function of exposure time constitutes a "ramp". The typical duration of a ramp is 32/250 s (or about 1/8 s), during which the telescope and instrument parameters remain fixed. The assignment to grating positions, chop phases, nod phases and map position is provided by information in the file header of the raw data. First, the pipeline splits up the grating positions and chop phases recorded in a single file, which represents only one map position and nod phase. The ramps are then fitted with linear slopes and are averaged for a single grating position and chop phase. Chop and nod subtractions are performed, and each of the 400 pixels is as signed with its spatial position and a wavelength. Flat fields are then applied. The flat fields are created from "sky dips", where the sky background is observed at two different telescope elevations to generate a signal without telescope and instrument background. For data obtained in Cycle 5 and later, flat fields taken

J. Astron. Instrum. 2018.07. Downloaded from www.worldscientific.com
by GERMAN AEROSPACE CENTER (DLR) on 01/09/19. Re-use and distribution is strictly not permitted, except for Open Access articles.

with the internal calibration source are available; these offer superior spectral coverage.The full spectral scans necessary to generate these are time consuming, but can be easily obtained in the lab, while time in-flight is very limited.

After combining the different grating positions within a file into a single spectrum, a telluric correction is also performed.With the relevant information from the file headers (flight altitude, telescope elevation) an ATRAN (Lord, 1992) transmission curve is calculated, convolved with the spectral resolution of the instrument and then used to correct the data. Since the data are not yet combined into a map, this allows one to account for changing flight altitudes and telescope elevations. However, this technique can be problematic near narrow atmospheric features since the convolution with the instrumental resolution significantly changes the shape of those features whereas the astronomical signal interacts with the unconvolved transmission profile of the atmosphere. Nevertheless, for many data sets this method has proven sufficient. If the transmission profile in the relevant spectral region does not allow for this method to be applied, telluric corrections can still be applied to the completed map using the following procedure.The astronomical signal is assumed to consist of an emission line a top a continuum that varies linearly with wavelength. A telluric transmission profile is applied to this signal and the result is convolved with the instrumental spectral resolution. This model is then fitted to the observed spectrum. Here the parameters of altitude and elevation have to be assumed constant throughout the map, or the map has to be split into smaller entities during which this assumption holds. If there is a sufficiently strong continuum source available in the mapping area and a telluric water line is covered within the wavelength range of the observations, this method can be used to estimate the water vapor content of the atmosphere at the time of the observations. This method has been successfully used for the telluric correction applied to data obtained from the galactic center (Iserlohe *et al.*, 2018).

To overcome the unavailability of a calibrated water vapor monitor, the FIFI-LS team has successfully tested a method to measure the water vapor with the instrument itself. In intervals of about 20 min the astronomical observations were paused, and several water lines close to the observed wavelength were measured in an unchopped manner. By choosing the right water lines, it was possible to create a setting sensitive to the water vapor content in the atmosphere. This technique creates an additional overhead of about 10% wall clock time and is suggested by the team for those observations where *a priori* investigation with an ATRAN modeled atmosphere shows the transmission to be sensitive to water vapor.

Both the telluric corrected as well as the uncorrected data cubes are available as pipeline products. The next reduction steps are the flux calibration and the bary-centric velocity correction. Since the data are not combined into a single cube yet, it is still possible to use different calibration curves (e.g. for different filter and dichroic configurations). Then the data are resampled onto a regular wavelength grid. Finally, the pipeline resamples each wavelength plane onto a regular spatial grid. This step combines the spatial information from all input nod-combined dither positions into a single output map with a smooth local polynomial surface fit. An example for data reduced with the FIFI-LS pipeline is shown in Fig. 1.

In-flight the pipeline is also used to create quick-look results of the observed data to enable real-time decisions on the observing strategy.

4. Performance

4.1. *Spectral resolution*

To verify the delivered spectral resolution of FIFI-LS on-sky, observations of the width of fine structure lines were taken toward the planetary nebulae NGC 7027 and NGC 6543 as well as the carbon star IRC+10216. The full width at half maximum intensity (FWHM) of those lines was then compared to the values obtained with the FIFI-LS telescope simulator in the laboratory (Colditz, 2017). Observations of calibration targets were taken on multiple flight series between April 2014 and March 2017.

The planetary nebulae proved ideal, since they feature bright narrow line emission and relatively low continuum flux levels. In these cases, the reduced data cube without telluric correction can be used for the analysis. The CO emission lines from IRC + 10216 offer access to even more wavelengths. Due to the strong underlying continuum for some wavelengths ($\sim$69 μm and 77 μm), the telluric corrected cube generated by the pipeline had to be used to obtain a first-order polynomial fit for the baseline. Each line is fitted with a Gaussian profile to

J. Astron. Instrum. 2018.07. Downloaded from www.worldscientific.com
by GERMAN AEROSPACE CENTER (DLR) on 01/09/19. Re-use and distribution is strictly not permitted, except for Open Access articles.

determine its FWHM. Pixels with an integrated line flux below a threshold of 10–50% of the peak integrated line flux are cut from the analysis since they are classified off-source. The median of the remaining values is used to create a data point. If a source/line was observed multiple times during a flight series, the data sets are evaluated separately. The results are shown in Fig. 6. Some scatter is present and it should be noted that the signal-to-noise ratio (SNR) is much higher for the gas cell measurements in the lab compared with those from the astronomical data, especially at 200 μm where the detectors sensitivity is quite low. Generally, the measurements confirm that FIFI-LS delivers the same spectral resolution in-flight as it does in the lab.

4.2. *Sensitivity*

The sensitivity of the instrument was verified in-flight as a by product to full range spectral scans of Mars that were primarily used to obtain the flux calibration of FIFI-LS. To obtain values for the sensitivity, the noise on a single ramp was evaluated without any chop or nod subtraction. The typical astronomical signal for FIFI-LS is usually below 1% of the background. This makes the chop and nod phase insignificant for the noise analysis. A single ramp represents an integration time of about 1/8 s. Then, the standard deviation of that ramp compared to the linear fit applied in the FIFI-LS data reduction is the noise in the signal.

The results are presented and compared to predictions from Klein *et al.* (2014) in Fig. 7. Shown are the results for both channels (red and blue) with the two orders (second order, 50 to 70 μm, and first order, 70 to 120 μm) in the blue channel. The left graph shows the minimum detectable continuum flux (MDCF) in Jy, and the right graph shows the minimum detectable line flux (MDLF) in 10^{-17} W/m^2. Both are scaled to 4σ in 15 min

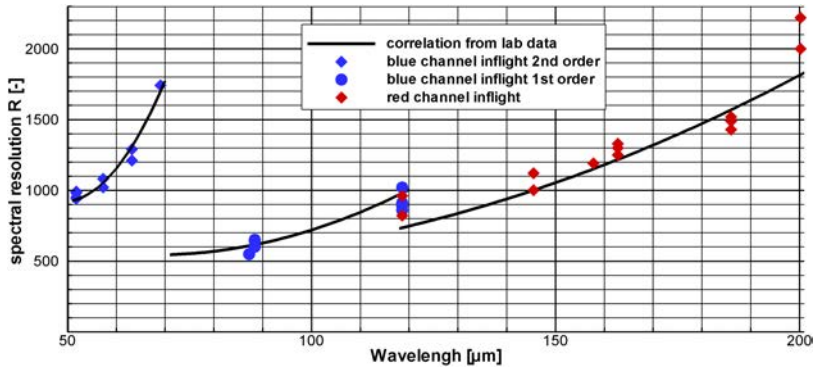

Fig. 6. Spectral resolution of the instrument in-flight compared to prediction from laboratory measurements. The solid black lines show the results from the laboratory measurements (Colditz *et al.*, 2018). The symbols show the verification measurements performed on sky.

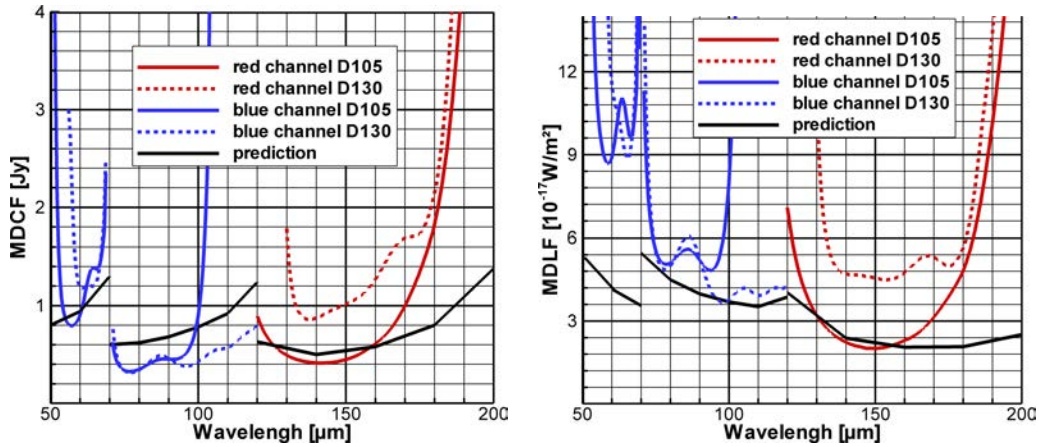

Fig. 7. Continuum (left) and line sensitivity (right) of FIFI-LS. Both are scaled to 4σ in 15 min on-source.

J. Astron. Instrum. 2018.07. Downloaded from www.worldscientific.com by GERMAN AEROSPACE CENTER (DLR) on 01/09/19. Re-use and distribution is strictly not permitted, except for Open Access articles.

on-source integration times. For most of the spectral coverage, data is shown for both dichroic beam splitters with a solid line for the D105 (cutoff at $\sim$105 μm) and a dashed line for the D130 (cutoff at $\sim$130 μm). Values are also scaled to the size of the FIFI-LS spaxels (6×6 arc sec^2 in the blue channel and $12\times$ 12 arc sec^2 in the red).

For the continuum sensitivity, it is assumed that the signal is averaged over the whole spectral coverage of the detector. The noise on a single pixel is divided by the square root of the number of resolution elements available within the spectral coverage of the detector. The number of resolution elements is calculated from the spectral resolution. For the line sensitivity, the noise on a single pixel is scaled to the FWHM of a narrow line. The predictions are based on noise estimates based on the temperatures of the optics of the telescope and the instrument, as well as the predicted spectral resolution.

The steep slopes of the sensitivity (both MDCF and MDLF) at the edges of the spectral coverage are caused by the rapidly decreasing transmission of the filters in the instrument. In the blue channel second order (50–70 μm) the continuum sensitivity matches the prediction for $\lambda >\sim 54\,\mu$m with the D105 dichroic and $\lambda >\sim 59\,\mu$m for the D130 dichroic. The higher wavelength cutoff of the D130 dichroic is not an issue for the observation setup, since it is primarily used to access longer wavelengths $\lambda >\sim 90\,\mu$m in the blue channel. In the first order, both dichroics show a similar performance up until about 90 μm where the filter curve of the D105 starts to drastically reduce transmission. The performance is significantly better than predicted caused by a change of the instantaneous spectral coverage of the blue channel late in development of FIFI-LS. For the red channel with the D105 dichroic, the performance meets or exceeds the prediction roughly between 125 μm and 160 μm with a decreased sensitivity for the D130 dichroic. The decreasing sensitivity for wavelengths about 160 μm is mainly caused by the decreasing grating efficiency and the rapidly decreasing detector sensitivity after above $\sim$190 μm.

The line sensitivity for the second order is about a factor of two lower than the prediction. This is caused by the spectral resolution being about a factor of two lower than originally anticipated (Colditz *et al.*, 2018). The important [OIII] line at 52 μm is located on the slope with rapidly decreasing sensitivity. To address this issue, a filter upgrade has been performed that doubles the transmission for the [OIII] line and improves the transmission in the whole second order by about 30%. The filters have been installed, the performance has been verified in the lab, and it a waits final in-flight verification. The line sensitivity in the first order of the blue channel ($\sim$70–120 μm) is close to the prediction with a dip around 85 μm. Since the spectral resolution for the red channel is within about 10% of the prediction, line and continuum sensitivity behave very similar relative to the prediction. This guarantees excellent performance for the two main red channel lines of [OI] at 146 μm and [CII] at 158 μm.

4.3. *Flux calibration*

The flux calibration of FIFI-LS was computed using observations of asteroids, planets and planetary moons. They are used, along with time-dependent models of such objects, to derive instrumental response curves. To date, observations of Mars have been used as the primary flux calibration source. Predicted total fluxes for Mars across the FIFI-LS passband at the specific UT dates of the observations have been generated using the model from Lellouch & Amri (2006).

In order to check the calibration, fluxes measured with FIFI-LS are compared with ISO LWS measurements from Liu *et al.* (2001). To account for the uncertainty of telluric correction, 50% is added to or subtracted from the standard zenith values of water vapor used by ATRAN (e.g. 7.3 μm precipitable water vapor at 41,000 ft). For the two [OI] lines at 63 μm and 146 μm, the telluric correction tool described above (Iserlohe *et al.*, 2018) has been used. For the other lines, which are farther away from telluric features, the line flux was fitted to the uncorrected result cubes and then divided by the transmission at the line location. The results for that comparison are shown in Table 2.

General agreement between FIFI-LS and ISO LWS is very good. We strongly suspect the [NIII] data taken on 2014 April 24 were affected by water vapor and +50% higher than the assumed value. The data showed a low SNR compared to the other [NIII] data from the same source with similar integration time. The 12 h weather updated flight plan predicted about 34 μm of zenith precipitable water vapor compared to the 11 μm used as maximum

J. Astron. Instrum. 2018.07. Downloaded from www.worldscientific.com
by GERMAN AEROSPACE CENTER (DLR) on 01/09/19. Re-use and distribution is strictly not permitted, except for Open Access articles.

Table 2. Overview over cross-calibration with FIFI-LS; the last two columns show the minimum and maximum flux relative to the ISO LWS values. The values are calculated using standard ATRAN water vapor −50% (maximum) and +50% (minimum).

λ [μm]	Line	Date [dd.mm.yyyy]	Source	Altitude [ft]	Av. elevation angle [°]	Min. flux relative to ISO LWS	Max. flux relative to ISO LWS
51.815	[OIII]	26.04.2014	NGC 7027	41,000	23	1.02	1.29
51.815	[OIII]	14.10.2015	NGC 6543	41,000	40	1.05	1.12
51.815	[OIII]	26.10.2015	NGC 6543	41,000	43	1.07	1.14
57.317	[NIII]	22.04.2014	NGC 7027	41,000	45	0.73	0.86
57.317	[NIII]	24.04.2014	NGC 7027	41,000	44	0.50	0.58
57.317	[NIII]	26.04.2014	NGC 7027	41,000	21	0.74	1.00
63.184	[OI]	20.10.2015	NGC 7027	43,000	39	0.87	1.36
63.184	[OI]	27.10.2015	NGC 7027	37,000	47	0.80	2.90
88.356	[OIII]	02.03.2016	NGC 6543	43,000	48	0.95	0.98
145.525	[OI]	26.04.2014	NGC 7027	41,000	23	0.60	0.96

value above. Using the predicted value to calculate an atmospheric transmission for the line, the maximum flux relative to ISO LWS increases to 1.25, indicating that this is the most likely explanation for the low measured flux for that flight.

Under the somewhat arbitrary assumption of +/− 50% for the minimum and maximum water vapor values, all but one measured flux values deviate from the ISO LWS values by less than 15%, a result which indicates good agreement between the FIFI-LS measured fluxes with those measured from space with ISO-LWS, and therefore confirms the overall flux calibration of the instrument.

4.4. *FIFI-LS and PACS*

FIFI-LS has a very similar design to the PACS instrument onboard the *Herschel* satellite. Since PACS is no longer operational, FIFI-LS is an ideal tool for follow-up observations. Since SOFIA is not a space telescope, FIFI-LS does not offer the sensitivity of PACS, but it does offer several features to bridge the sensitivity gap and enable observations not feasible with PACS:

- FIFI-LS employs two complete, and completely independent, spectrometer channels, whereas PACS used only one over the entire wavelength range. This difference enables simultaneous observations of two individually selectable spectral lines with FIFI-LS, which increases FIFI-LS's observing efficiency significantly. In the PACS spectrometer, the wavelengths in the two channels are interdependent — bound by the common grating — and are not individually selectable.
- Due to the two independent grating channels in FIFI-LS, the useful wavelength range of FIFI-LS (51–200 μm) exceeds that of PACS (55–200 μm). FIFI-LS can observe additional diagnostic lines, especially the [OIII] line at 51.815 μm.
- The pixel size in the PACS spectrometer, as set by the one IFU, is 9.4″, which is optimum in the long wavelength part of the instrument, but noticeably under-samples the telescope PSF at shorter wavelengths. As FIFI-LS uses two independent IFUs, one for each channel, the projected pixel sizes are 12″ in the red channel and 6″ in the blue channel, providing FIFI-LS with a better angular resolution in the short wavelength range (51 μm$\sim$120 μm) compared with PACS, even though *Herschel* provides a larger effective telescope aperture.
- The spectral resolution of the two instruments is comparable, but the execution time per observation and the sensitivities differ. The "raw" sensitivity (point source, unresolved spectral line) of *Herschel*/PACS is about eight times better than that of SOFIA/FIFI-LS, owing to the lower telescope temperature and emissivity, the lack of atmospheric emission and absorption, and the larger telescope diameter. The "atomic building block" of a PACS observation executes in $\sim$7 min, after which time the noise in a line-detection is $\sim 3 \times 10^{-18}$ W/m^2. For deep observations, this is a useful building block, of which a number of repetitions can be executed to reach the desired depth (SNR). However, for (fully sampled) mapping of sufficiently bright, large objects (e.g. nearby galaxies), this leads to very long integration times and highly "over-integrated" line-detections (e.g. SNR values > 100), which are then limited by systematic effects and calibration precision. Here SOFIA/FIFI-LS

J. Astron. Instrum. 2018.07. Downloaded from www.worldscientific.com by GERMAN AEROSPACE CENTER (DLR) on 01/09/19. Re-use and distribution is strictly not permitted, except for Open Access articles.

has an advantage, since the telescope time to move from pointing to pointing on the sky is only about 8 s on average. This enables fast mapping of relatively bright sources. In the symmetric chop mode the minimum on-source integration time typically used with FIFI-LS is 30 s, with a total wall-clock time of about 75 s. FIFI-LS has already successfully carried out mapping projects of M51 (noise $\sim$1.6 W/m^2 in $\sim$15 h total wall clock time) and NGC6946 (noise $\sim$2.3 W/m^2 in $\sim$10 h wall clock time).

- For mapping extended targets (e.g. nearby galaxies) in several spectral lines, the capability to observe two lines simultaneously with the faster and more efficient observing scheme provides FIFI-LS with a multiplex advantage of more than a factor of two. FIFI has done this successfully for galactic and extragalactic sources. For example, FIFI-LS has created maps of the [OI] lines at 63.184 μm and 145.525 μm, covering an area of 32.5 arc min^2 in 130 tiled fields in about 75 min of wall-clock time.

5. Observing with FIFI-LS

5.1. *Observing modes*

To subtract the high background present in far-infrared observations, FIFI-LS uses chopping of the telescope secondary for all standard observing modes. The typical chop frequency for FIFI-LS is $\sim$2 Hz. Only about 3.1% of the integration time is affected by the chopper transition at this frequency, which has proven to be sufficiently fast for the quickly changing weather conditions and climbs of the aircraft during flights. Since the two chop beams use different portions of the primary mirror, nodding is used to subtract the residual background. FIFI-LS offers three different standard observing modes to general observers:

- Symmetric chop,
- Asymmetric chop,
- Bright object mode.

The most commonly-used mode is the symmetric chopping mode. It is also the most efficient one, since in symmetric chopping, also known as beam switching, the source is present in one chop phase for both nod positions (A and B). Overheads are created by the time spent in off chop phase and by the time the telescope takes to switch between nod beams and/or map positions. For symmetric chopping FIFI-LS uses an on-source nod time of 30 s, which results in a nod efficiency of about 80% if one also accounts for the average telescope move time of 8 s. The efficiency degrades quickly for shorter nod dwells and improves only very slowly for longer nod dwell times (Fischer *et al.*, 2016). Symmetric chopping does create a coma effect that limits the total chop-throw to 5–8 arc min in the FIFI-LS wavelength range and requires an area free of astronomical signal at the chop angle as well as in the opposite direction. If symmetric chop is not possible, an asymmetric chop can be considered allowing for a total chop throw of up to 10 arc min and requiring an emission free area only in the direction of the chop, since the nod can be performed in areas much further away in the sky. The downside of that mode is that only 25% of the total integration time is spent on the source cutting the observing efficiency in half to about 20%.

Some of that loss can be recovered by using the bright object mode, where an identical grating setup is used on all integrations, thus limiting the spectral width available to roughly the instantaneous spectral coverage (Klein *et al.*, 2014). Here one "off nod" (B) is used for multiple "on nods" (A) in an ABA (30 s on nod) or AABAA (20 s on nod) scheme. The latter being the fastest mapping mode available with FIFI-LS. Such a strategy pushes the efficiency closer to the symmetric chopped mode. This mode is also the fastest available for very bright sources, since it allows shorter integration times per map position (down to 10 s on-source) compared to symmetric chopping (30 s on-source). If the observed spectral line of a weaker source does not require a wide spectral scan, this mode can also be used for deep integrations.

The feasibility of an unchopped "total power" mode has also been investigated using an on-source integration time of 10 s in an ABA scheme. With an efficiency of 37% this mode almost reaches the efficiency of the symmetric chopped mode (39%). It is also superior to the asymmetric modes with their efficiency of 20–29%. For comparison, the same map has been acquired with the bright object mode on the same flight with the same on-source integration time. The analysis of the test data showed a comparable but lower data quality for the total power mode. There is also a higher risk associated with those observations since background fluctuations are subtracted about 100 times slower compared to chopped observations. Also the aircraft cannot

J. Astron. Instrum. 2018.07. Downloaded from www.worldscientific.com
by GERMAN AEROSPACE CENTER (DLR) on 01/09/19. Re-use and distribution is strictly not permitted, except for Open Access articles.

climb during those observations. Still the mode is available and feasible for those observations otherwise showing a high risk of self-chopping in crowded fields on the sky. Also, existing chopped observations have been reduced "total power style" when there were indications of self-chopping. This did result in some loss of SNR, but still enabled scientific interpretation of the data.

For observation planning with FIFI-LS, the SOFIA USPOT tool is available to set up and visualize the observations.[a] This includes the spectral setup, chop and map/dither. Some instrument specific observation parameters and the observing strategy are then later developed by the SOFIA support scientist together with the observer, once the proposal has been accepted. FIFI-LS has multiple recommended map/dither schemes that can be found in Fischer *et al.* (2016). An observation time estimator based on the noise performance and the overheads mentioned above is available online.[b]

5.2. *Data analysis tools*

Multiple tools to analyze the data are available for the community online.[c] Available are tools for cube exploration (SOSPEX) line and continuum fitting (FLUXER) and a fitting tool for telluric correction. FLUXER was used to extract the line and continuum flux shown in Fig. 1.

6. Conclusion and Outlook

With FIFI-LS, a unique and versatile instrument has been added to the SOFIA observatory. It can very quickly map bright and large galactic line and continuum sources of bright galactic sources and provides the sensitivity to augment existing data sets of, e.g., the PACS instrument with further spectral transitions or to explore new extragalactic targets. Since it has been offered to the community in 2015, there has been a constantly high demand for FIFI-LS with about 30 proposals for every observing cycle.

All aspects of the instrument as well as the way to utilize it are constantly under development. The water vapor measurement is the latest improvement to the operation of FIFI-LS. Both the instrument control software as well as the pipeline are constantly updated with bug fixes and other improvements as well.

For Cycle 6 in 2018, the hardware of FIFI-LS was updated for the first time with a new entrance filter and new order sorter filters for the blue channel to improve the sensitivity for numerous lines in the blue channel. Currently, there is also a major upgrade under investigation for FIFI-LS to increase the spatial and instantaneous spectral coverage of the instrument and potentially widen the spectral range to continue to improve the efficiency of FIFI-LS on SOFIA.

[a] https://dcs.arc.nasa.gov/observationPlanning/install-USPOT/uspotDownload.jsp.
[b] https://dcs.arc.nasa.gov/.
[c] https://www.sofia.usra.edu/science/proposing-and-observing/data-products/data-resources.

Acknowledgments

SOFIA, the "Stratospheric Observatory for Infrared Astronomy" is a joint project of the DeutschesZentrumfürLuft- und Raumfahrte.V. (DLR; German Aerospace Center, grant: 50OK0901) and the National Aeronautics and Space Administration (NASA). It is funded on behalf of DLR by the Federal Ministry of Economics and Technology based on legislation by the German Parliament, the state of Baden-Württemberg and the Universität Stuttgart. Scientific operation for Germany is coordinated by the German SOFIA Institute (DSI) of the Universität Stuttgart, in the USA by the Universities Space Research Association (USRA).

The team would like to thank the SOFIA observatory including NASA, USRA, DLR and DSI. The eight FIFI-LS flight series conducted up to the time of writing were successful only due to the excellent cooperation of all participants.

References

Bryant, A., Fischer, C., Hönle, R. *et al.* [2014] "FIFI-LS observation planning and data reduction," *Proc. SPIE* **9147**, 91474C.

Clarke, M., Vacca, W. D. & Shuping, R. Y. [2015] "*Redux: A Common Interface for SOFIA Data Reduction Pipelines*," ADASS, ASP Conference Series, Vol. 495, 355.

Colditz, S., Klein, R., Beckmann, S. *et al.* [2014] "Boresight Calibration of FIFI-LS: in theory, in the lab and on sky," *Proc. SPIE* **9147**, 91474S.

Colditz, S. [2017] "FIFI-LS – A Field-Imaging Far-Infrared Line Spectrometer for SOFIA: Completion of the Instrument, Laboratory and In-flight Calibration and Characterization," (Dr. Hut Verlag), Dissertation, University of Stuttgart, Germany.

Colditz, S., Beckmann, S., Bryant, A. *et al.* [2018] "Spectral and spatial characterization and calibration of FIFI-LS — The

field imaging spectrometer on SOFIA," *J. Astron. Instrum* **7**, 1840004.

Erickson, E. F. & Davidson, J. A. [1993] "SOFIA: Stratospheric Observatory for Infrared Astronomy," *Adv. Space Res.* **13**(12), 549–556.

Fischer, C., Bryant, A., Beckmann, S. *et al.* [2016] "Observing with FIFI-LS on SOFIA: Time estimates and strategies to use a field imaging spectrometer on an airborne observatory," *Proc. SPIE* **9910**, 991027.

Guesten, R., Camara, I., Hartogh, P. *et al.* [2003] "GREAT: The German Receiver for Astronomy at Terahertz Frequencies," *Proc. SPIE* **4857**, doi: 10.1117/12.458820.

Iserlohe, C., Bryant, A., Krabbe, A. *et al.* [2018] "FIFI-LS observations of the Circumnuclear Ring, Probing the high-density phase of the PDR," to appear in *ApJ.*

Kessler, M. F., Steinz, J. A., Anderegg, M. E. *et al.* [1996] "The Infrared Space Observatory (ISO) mission," *A&A* **315**, L27–L31.

Klein, R., Poglitsch, A., Fumi, F. *et al.* [2004] "Real-time operation without a real-time operating system for instrument control and data acquisition," *Proc. SPIE* **5496**, doi: 10.1117/12.551111.

Klein, R., Beckmann, S., Bryant, A. *et al.* [2014] "FIFI-LS: the facility far-infrared spectrometer for SOFIA," *Proc. SPIE* **9147**, 91472X.

Lellouch, E. & Amri, H. [2006] *Mars brightness model*, http://www.lesia.obspm.fr/perso/emmanuel-lellouch/mars/index.php.

Liu, X.-W., Barlow, M. J., Cohen, M. *et al.* [2001] "ISO LWS observations of planetary nebula fine-structure lines," *MNRAS* **323**, 343.

Looney, L. W., Geis, N., Genzel, R. *et al.* [2000] "Realizing 3D spectral imaging in the far-infrared: FIFI LS," *Proc. SPIE* **4014**, doi: 10.1117/12.389112.

Looney, L. W., Klein, R. *et al.* [2018] *First Look at Orion-KL with FIFI-LS onboard SOFIA*, to appear.

Lord, S. D. [1992] NASA Technical Memorandum 103957.

Nagao, T., Maiolino, R., Marconi, A., Matsuhara, H., [2011] "Metallicity diagnostics with infrared fine-structure lines," *A&A* **526**, A149.

Poglitsch, A., Waelkens, C., Geis, N. *et al.* [2010] "The Photodetector Array Camera and Spectrometer (PACS) on the Herschel Space Observatory," *A&A* **518**, L2.

Raab, W., Looney, L. W., Poglitsch, A. *et al.* [2003] "FIFI LS: the optical design and diffraction analysis," *Proc. SPIE* **4857**, 91474G.

Rebell, F., Raab, W., Colditz, S. *et al.* [2014] "Precise angular positioning at 6K: the FIFI-LS grating assembly," *Proc. SPIE* **9147**, 914735.

Rebell, F., [2018] "Laboratory characterisation of FIFI-LS cryogenic subsystems and their in-flight performance onboard SOFIA," to appear.

Rosenthal, D., Beeman, J. W., Geis, N. *et al.* [2000] "16 x 25 Ge:Ga detector arrays for FIFI LS," *Proc. SPIE* **4014**, doi: 10.1117/12.389096.

Schweitzer, M. [2008] "Optical Alignment and Characterization of FIFI-LS — The Field-Imaging Far-Infrared Line Spectrometer," Dissertation of the faculty of physics of the Ludwig-Maximilian-University Munich.

Stutzki, J. [2004] "Sub-mm-instrumentation: Current projects at KOSMA/Universität zu Köln," *Proc. SPIE* **5498**, doi: 10.1117/12.555951.

Thompson, R. [2011] *User Manual for the Telescope Assembly Alignment Simulator*, SOFIA Program, SCI-AR-MAN-OP02-2068.

J. Astron. Instrum. 2018.07. Downloaded from www.worldscientific.com
by GERMAN AEROSPACE CENTER (DLR) on 01/09/19. Re-use and distribution is strictly not permitted, except for Open Access articles.